

Three Dimensional Reconstruction of Blood Vessels from Stereoscopic Magnetic Resonance Angiography

Jan-Ray Liao* Shye-Chorng Kuo Lei-Shin Kuo Shi-Hui Huang Jeng-Jye Jou

Department of Electrical Engineering, National Chung Hsing University, Taichung, 402, Taiwan, R.O.C.

Received 1 May 2004; Accepted 10 June 2004

Abstract

Magnetic resonance angiography (MRA) was an imaging technique to show the blood vessels but suppress signals from all the other tissues. There were two approaches to acquire an image of MRA. One was done in two-dimension (2-D) by projecting the three-dimensional (3-D) vessels onto 2-D plane. The other was to directly obtain the complete 3-D information. The advantage of 3-D MRA was that one can view the data from arbitrary direction. However, the scan time was usually very long for 3-D MRA. When the scan time was limited, we must use 2-D MRA and the depth information was lost. The depth information could be partially recovered using stereoscopic angiography, i.e., acquiring two 2-D images from different viewing angles. In addition to the stereoscopic views, stereoscopic angiography could also be used to reconstruct the 3-D shapes of the vessels. However, 3-D reconstruction was used more frequently in digital subtraction X-ray angiography (DSA). The main reason was that pixel intensity was directly related to the integration of the attenuation value along the path of the X-ray in DSA. Therefore, we could derive the vessel shape by solving the integrals from the two views. On the other hands, there were many imaging parameters in MRA (T1, T2, and proton density). Therefore, it was difficult to obtain the relation between the vessel shape and the pixel intensity. For this reason, we attempted to reconstruct the shape of the vessels simply from the edge information of the two views. We assumed that the shape of the vessel on every cross-section was an ellipse. Then, we developed an algorithm to estimate the parameters of the ellipse from the boundaries of the projective images. A 3-D MRA data set was used to test the capability of our algorithm. From these data, we made two projective images. The two projections were 30° apart. We employed our algorithm to estimate all the ellipses and reconstruct the 3-D model of the vessels. Comparing the boundaries of the original projective images with the boundaries of the reconstructed 3-D model, the average error was 0.1011 pixels.

Keywords: Magnetic resonance angiography, Stereoscopic angiography, Three-dimensional reconstruction, Blood vessel geometry

Introduction

Angiography was a technique to show the blood vessels. Magnetic resonance angiography (MRA) [1, 2] achieved this goal by designing imaging sequence to enhance the signals from blood inside the vessels and suppress the signals from the surrounding static tissues. A typical MRA image was shown in Fig. 1. Because there were many parameters that we could use in magnetic resonance imaging (MRI), there were many methods for MRA, for example: time-of-flight MRA [3], digital subtraction MRA[4], flow-independent MRA[5], and phase-contrast MRA [6]. In terms of the dimension of the data we acquired, MRA could be divided into two categories: two-dimensional MRA(2-D MRA) and three-dimensional MRA (3-D MRA). In 2-D MRA, the image was obtained as

the two-dimensional projection of the three-dimensional volume. The benefit of 2-D MRA was its short scan time but the drawback was that spatial information on the third dimension (depth) was lost. On the contrary, 3-D MRA collected the whole three-dimensional data. There were two ways to do so. One was by stacking thin slices into 3-D volume. The other was by directly traversing the complete 3-D k-space. Having the 3-D data, we could then project the 3-D data to any angle we want to observe. The price we pay to get this flexibility was the much longer scan time than that of 2-D MRA. And, because of the long scan time, other motion such as heartbeat and breath was very likely to cause artifacts in the images. Therefore, 3-D MRA was difficult to use in regions susceptible to the influence of motion.

In traditional X-ray imaging, stereoscopic angiography [7] was invented to overcome the problem that 2-D angiography lacks depth information. The theory of stereoscopic angiography was simple. The original 2-D angiography was

*Corresponding author: Jan-Ray Liao
Tel: +886-4-22851549 ext, 271; Fax: +886-4-22851410
E-mail: jrliao@mail.nchu.edu.tw

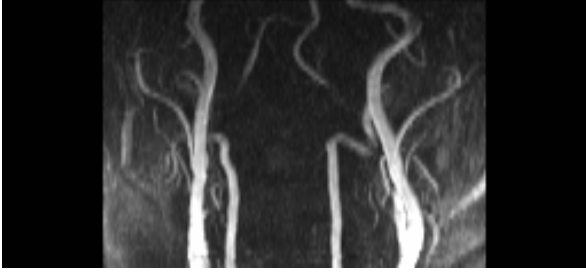


Fig. 1 A typical maximum-intensity-projection MRA image.

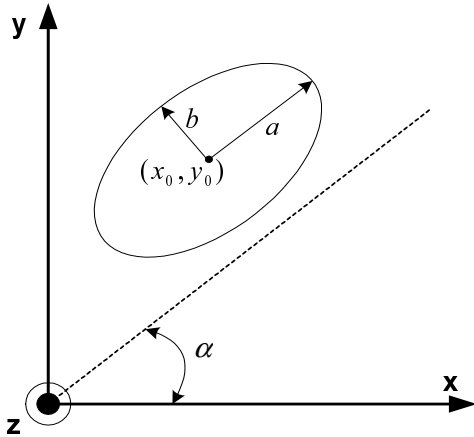


Figure 2. A depiction of the coordinate system and the ellipse to be estimated.

looking straight down the slice in the direction perpendicular to the observed plane. By rotating the observation angle slightly to the left and right, we created two images with slightly different viewing angles. The result was a pair of stereoscopic images in which we could differentiate the depth of the objects. Although the scan time was doubled, it was still short compared to 3-D acquisition. So, stereoscopic angiography had the advantage of faster scan time while still preserving depth information. Theoretically, we could recover the depth information of the vessels from the two projections at different viewing angles. For X-ray DSA, the pixel intensity was directly related to the integration of the attenuation value in the path of the X-ray. We could derive the vessel shape by solving the integrals from the two views [8-18]. On the other hands, there were many imaging parameters in MRA (such as T_1 , T_2 , and proton density). Therefore, it was difficult to obtain the relation between the vessel shape and the pixel intensity. In this paper, we proposed a new method to reconstruct the shape of the vessels from the edge information only.

Methods

3-D Reconstruction Algorithm

For the ease of discussions below, we used a coordinate system where x was from left to right, y was away from the viewer, and z was from top to bottom. The coordinate system was independent of the projection angle. After rotating $\theta/2$ angles to both left and right, two projections were taken as the stereoscopic images.

The basic assumption we made was that blood vessels were all circular tubes. One might argue that this was a very restrictive assumption. However, we believed that the application of the 3-D reconstruction algorithm was to aid the radiologists to make decisions on how to do additional scans instead of using it for diagnosis directly. Therefore, although the assumption might not be true in general, it provided a foundation to estimate the 3-D model quickly and should be useful in practice.

Furthermore, we assumed that the blood vessel was not tilting from the z -axis for more than 45 degrees. When a vessel did not match this constraint, we could rotate the coordinate system to make it satisfy this assumption. When a circular tube was tilted, its cross section became an ellipse. The goal of the algorithm was to reconstruct the ellipse from the edges of the two stereoscopic images. Before discussing the reconstruction algorithm, we needed to establish some basic mathematical relationships between the ellipse and its projection.

1. Expressing an ellipse in matrix form:

An ellipse with its center at the origin could be expressed as follows [19]:

$$[x \ y] X^{-1} \begin{bmatrix} x \\ y \end{bmatrix} = 1 \tag{1}$$

where X was a 2×2 positive semi-definite matrix,

$$X = \begin{bmatrix} A & B \\ B & D \end{bmatrix} \tag{2}$$

2. Relationship between the projection length and the matrix form:

Let vector C be an orthonormal basis for the projection plane. The relationship between the projection length and the matrix X was as follows [20]:

$$C^T = [u \ v] \tag{3}$$

$$Y = C^T X C \tag{4}$$

If we let the projection length of the ellipse be L , Y was equal to $(L/2)^2$. The easiest way to appreciate this result is to consider a circle where A must be equal to D . For the circle, it could be easily seen that Y was the square of the radius.

Plugging Equation (2) into Equation (4), we could obtain the relationship between X and Y as below:

$$Y = Au^2 + 2Buv + Dv^2 \tag{5}$$

With the above equations, we could now consider how to reconstruct the ellipse from projections. The task was essentially to find the center of the ellipse: x_0 and y_0 , the length of the long axis and short axis: a and b , and the angle of rotation α . These five parameters were shown in Fig. 2. We could describe the algorithm to find the five parameters from the two projections in three steps:

Step 1: Deriving the center of the ellipse:

Let x_{L1} and x_{L2} be the two edges from the left view. Let x_{R1} and x_{R2} be the two edges from the right view. The center of the ellipse was the intersection point of the two lines which

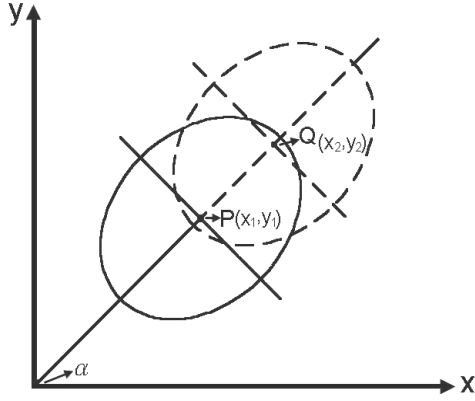


Figure 3. The relationship between adjacent slices. P and Q are the center of the two ellipses.

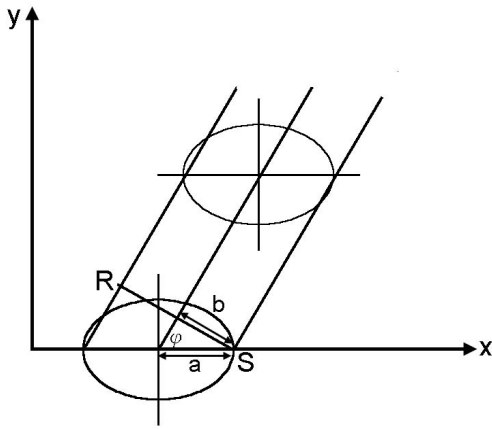


Figure 4. Tilting angle φ and two adjacent ellipses.

were coming from the middle points of the two views and perpendicular to the projection planes. Let x_0 and y_0 be the center. Then,

$$\begin{cases} x_0 = \frac{x_{Rm} + x_{Lm}}{2 * \cos \theta} \\ y_0 = \frac{x_{Rm} - x_{Lm}}{2 * \sin \theta} \end{cases} \quad (6)$$

Step 2: Deriving the rotation angle α :

Given the two pairs of edges in the stereoscopic images, there were infinite sets of ellipses that satisfied the constraints. If we looked down from the z-axis, it could be observed from Fig. 3 that the rotation angle of the ellipse was equal to the angle of the vector formed by connecting the center of the two ellipses on adjacent slices. Let α be the rotation angle, (x_1, y_1) and (x_2, y_2) be the centers of the two adjacent ellipses. We could write the following relationship:

$$\alpha = \tan^{-1} \left| \frac{y_1 - y_2}{x_1 - x_2} \right| \quad (8)$$

Step 3: Deriving long axis a and short axis b :

Since the ellipse we were estimating was resulting from a tilting circular tube, the length of the short axis b was equal to the radius of the circular tube. In the mean time, the long axis could be obtained from the tilting angle of the circular

tube as shown in Fig. 4. Let φ be the tilting angle. We knew that

$$a/b = (\sin \varphi)^{-1} \quad (7)$$

With the above relationship, we needed a second equation in order to solve for a and b . Given the rotation angle α obtained from step 2, we could write the elliptical equation as follows:

$$\begin{cases} x' = x \cos \alpha - y \sin \alpha \\ y' = x \sin \alpha + y \cos \alpha \end{cases} \quad (9)$$

$$\frac{(x')^2}{a^2} + \frac{(y')^2}{b^2} = 1 \quad (10)$$

Plugging Equation (9) into Equation (10), the resulting equation was equal to Equation (2) and we could equate the corresponding coefficients in the two equations to obtain the following simultaneous equations:

$$\begin{cases} A = a^2 - (a^2 - b^2) \sin^2 \alpha \\ B = -(a^2 - b^2) \cos \alpha \sin \alpha \\ D = b^2 + (a^2 - b^2) \sin^2 \alpha \end{cases} \quad (11)$$

Since the two projections were symmetric, the unit vector of the right projection plane was $C^T = [u \ v]$ and the unit vector of the left plane was $C^T = [-u \ v]$. From Equation (5), we could obtain the following two equations for the projection length.

$$\begin{cases} Y_r = u^2 A + 2uvB + v^2 D \\ Y_l = u^2 A - 2uvB + v^2 D \end{cases} \quad (12)$$

where Y_r was a quarter of the square of the right projection length and Y_l was a quarter of the square of the left projection length. Y_r and Y_l could be estimated from the edges of the projection vessel.

From Equation (12), we could obtain the following two equations:

$$B = \frac{(Y_r - Y_l)}{4uv} \quad (13)$$

$$u^2 A + v^2 D = (Y_r + Y_l)/2 \quad (14)$$

Combining the Equations (7), (11), and (14), we obtained the following simultaneous equations.

$$\begin{cases} A = a^2 - (a^2 - b^2) \sin^2 \alpha \\ D = b^2 + (a^2 - b^2) \sin^2 \alpha \\ u^2 A + v^2 D = (Y_r + Y_l)/2 \\ a/b = (\sin \varphi)^{-1} \end{cases} \quad (15)$$

Solving the above equations, we could obtain A and D . Substituting A , B , and D in X (Equation (2)), we could find the eigenvalues and eigenvectors of the matrix X . The maximum eigenvalue corresponded to the square of the long axis a and the direction of eigenvector was the direction of the long axis. Meanwhile, the minimum eigenvalue and its eigenvector corresponded to the square of the short axis b and its direction. Consequently we could successfully reconstruct the ellipse.

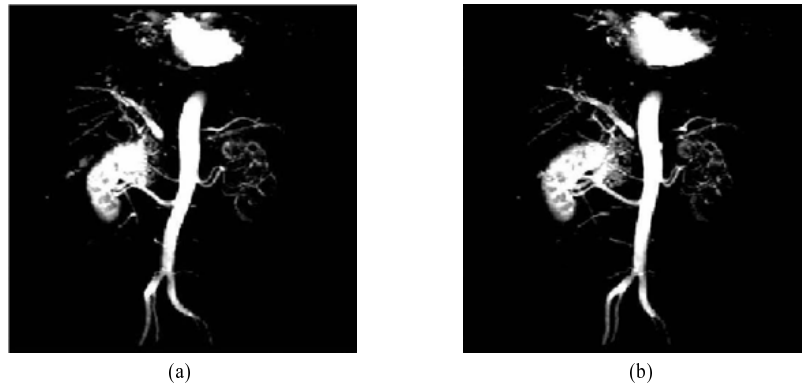


Figure 5. Stereoscopic MRA images: (a) left, (b) right.

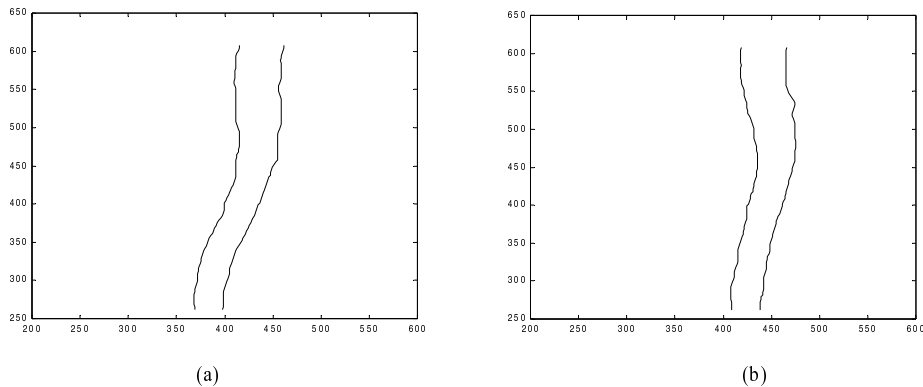


Figure 6. Detected edges of the (a) left view and (b) right view.



Figure 7. The reconstructed 3-D blood vessels

Edge Detection

Since the above algorithm required the edges of the two projections as the input, we used a graph-searching method [21] to detect the edges of the vessels. The projection was first processed by Sobel operator [22]. The processed image was used as the weights of the edges. The starting point and the end point of the vessel edge was then marked by a human operator. From the starting point to the end point, a path that maximized the sum of the weights was searched and taken as the inputs to the reconstruction algorithm.

Results

We used a 3-D MRA data set to test our algorithm. The 3-D data were acquired by stacking slices together on a 1.5T MRI scanner (GE Medical Systems, Milwaukee, Wisconsin). The scanning parameters were field-of-view: 40×40 (cm), resolution: 256×256 (pixels), slice thickness: 8 (mm), and total number of slices: 50. The $x-z$ plane is on the imaging plane and the y axis is along the direction where slices are stacked. The data set was projected along the y direction by rotating 15° left and right. The stereoscopic images were shown in Fig. 5.

The vessel edges were automatically traced out using the method previously discussed. Since the detected edges were integer values and looked a little jagged, we smoothed the edges with a hamming window of width 7. The vessel edges after smoothing were shown in Fig. 6.

We used the vessel edges to reconstruct the 3-D vessel shape. The reconstructed vessel was displayed in 3-D using OpenGL and was shown in Fig. 7. The reconstructed vessel was re-projected back to the original planes and compared to the input edges. The comparisons were shown in Fig. 8.

Subtracting the re-projected edges with the input edges and taking the absolute value, the error was 0.1131(pixels) for the left view and 0.0957(pixels) for the right view. The average of the absolute difference was approximately 0.1011(pixels).

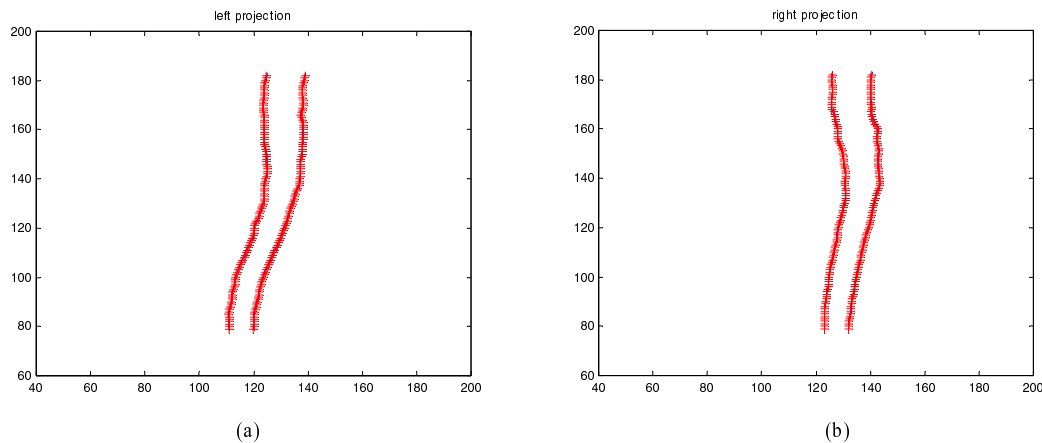


Figure 8. Reprojection of the reconstructed ellipses: (a) the left view, (b) the right view.

Conclusion

From these results, we had successfully demonstrated the reconstruction of 3-D vessels from only the edge information of the stereoscopic images. There were two directions to improve the current results. Since the reconstruction results depended heavily on the edge detection, improving the edge detection algorithm was a very important area for the future. In the mean time, how to reduce the error of the reconstructed vessels was also a very important direction for future research.

Acknowledgement

This work was supported by the National Science Council of the Republic of China under Contracts NSC-88-2213-E-005-025 and NSC-90-2213-E-005-027. We would also like to thank Dr. Jyh-Wen Chai (Department of Radiology, Taichung Veterans General Hospital, Taichung, Taiwan) for providing the 3-D MRA data to us.

References

- [1]. V. J. Wedeen, R. A. Meuli, R. R. Edelman, S. C. Geller, L. R. Frank, T. J. Brady, B. R. Rosen, "Projective imaging of pulsatile flow with magnetic resonance," *Science*, 230: 946-948, 1985.
- [2]. D. Atkinson, L. Teresi, "Magnetic resonance angiography," *Mag. Reson. Quarterly*, 10: 149-172, 1994.
- [3]. D. G. Nishimura, A. Macovski, J. M. Pauly, S. M. Conolly, "MR angiography by selective inversion recovery," *Magnetic Resonance in Medicine*, 4: 193-202, 1987.
- [4]. M. R. Prince, "Gadolinium-enhanced MR aortography," *Radiology*, 191: 155-164, 1994.
- [5]. J. H. Brittain, B. S. Hu, G. A. Wright, C. H. Meyer, A. Macovski, D. G. Nishimura, "Coronary angiography with magnetization-prepared T2 contrast," *Mag. Reson. Med.*, 33: 689-696, 1995.
- [6]. C. L. Dumoulin, H. R. Hart Jr., "Magnetic resonance angiography," *Radiology*, 161: 717-720, 1986.
- [7]. J. Kleefield, G. V. O'Reilly, J. B. Barsotti, M. L. Brooks, "Biplane Stereoscopic Magnification Cerebral Angiography," *Radiology*, 165: 576-577, 1987.
- [8]. Y. Bresler, A. Macovski, "Three-dimensional reconstruction from projections with incomplete and noisy data by object estimation," *IEEE Trans. Acoust., Speech, Signal Processing*, 35: 1139-1152, 1987.
- [9]. K. Kitamura, J. M. Tobis, J. Sklansky, "Estimating the 3-d skeletons and transverse areas of coronary arteries from biplane angiograms," *IEEE Trans. Med. Imaging*, 7: 173-187, 1988.
- [10]. Y. Bresler, J. A. Fessler, A. Macovski, "A bayesian approach to reconstruction from incomplete projections of a multiple object 3d domain," *IEEE Trans. Pattern Analysis Machine Intelligence*, 11: 840-858, 1989.
- [11]. J. A. Fessler, A. Macovski, "Object-based 3-d reconstruction of arterial trees from magnetic resonance angiograms," *IEEE Trans. Med. Imaging*, 10: 25-39, 1991.
- [12]. M. Garreau, J. L. Coatrieux, R. Collorec, C. Chardenon, "A knowledge-based approach for 3-d reconstruction and labeling of vascular networks from biplane angiographic projections," *IEEE Trans. Med. Imaging*, 10: 122-131, 1991.
- [13]. C. Pellot, A. Herment, M. Sigelle, P. Horain, P. Peronneau, "Segmentation, modelling and reconstruction of arterial bifurcations in digital angiography," *Medical & Biological Engineering & Computing*, 30: 576-583, 1992.
- [14]. L. van Tran, R. C. Bahn, J. Sklansky, "Reconstructing the cross sections of coronary arteries from biplane angiograms," *IEEE Trans. Med. Imaging*, 11: 517-529, 1992.
- [15]. C. Pellot, A. Herment, M. Sigelle, P. Horain, H. Maitre, P. Peronneau, "3D reconstruction of vascular structures from two x-ray angiograms using an adapted simulated annealing algorithm," *IEEE Trans. Med. Imaging*, 13: 48-60, 1994.
- [16]. S. Ruan, A. Bruno, J. L. Coatrieux, "Three-dimensional motion and reconstruction of coronary arteries from biplane cineangiography," *Image and Vision Computing*, 12: 683-689, 1994.
- [17]. A. Wahle, E. Wellnhofer, I. Mugaragu, H. U. Sauer, H. Oswald, E. Fleck, "Assessment of diffuse coronary artery disease by quantitative analysis of coronary morphology based upon 3-d reconstruction from biplane angiograms," *IEEE Trans. Med. Imaging*, 14: 230-241, 1995.
- [18]. J.-K. Guo, C.-H. Chen, J.-D. Lee, J.-M. Tsai, "3-d image reconstruction of brain blood vessels from angiograms," *Computers & Math. with Applications*, 35: 79-94, 1998.
- [19]. William C. Karl, George C. Verghese, and Alan S. Willsky, "Reconstructing Ellipsoids from Projections," *CVGIP: Graphical Models and Imaging Processing*, 56: 145-139, 1994.
- [20]. W. C. Karl, Reconstructing Objects from Projections, PhD thesis, Massachusetts Institute of Technology, Department of Electrical Engineering and Computer Science, Jan. 1991.
- [21]. S. R. Fleagle, R. R. Johnson, C. J. Wilbright, D. J. Skorton, R. F. Wilson, C. W. White, M. L. Marcus, S. M. Collins, "Automated analysis of coronary arterial morphology in cineangiograms: geometric and physiologic validation in humans," *IEEE Trans. Med. Imaging*, 8: 387-400, 1989.
- [22]. I. Sobel, "Neighborhood coding of binary images for fast contour following and general binary array processing," *Computer Graphics and Image Processing*, 8: 127-135, 1978.